NON-INVASIVE DRY ELECTRODES FOR EEG

M.F. Silva, N.S. Dias, A.F. Silva, J.F. Ribeiro, L.M. Goncalves, J.P. Carmo, P. M. Mendes, J.H. Correia

University of Minho, Dept. Industrial Electronics, Campus Azurem, 4800-058 Guimaraes, Portugal

***Abstract* - This paper presents a non-invasive dry electrode for electroencephalogram (EEG) acquisition. These electrodes can be integrated in a wearable braincap for wireless EEG that can be used for a long time by patients avoiding the contact gel. This wearable braincap will allow mobility to the patients, while simultaneously having their electrical brain activity monitored. The fabricated dry electrodes are based on iridium oxide (IrO_x) deposited by reactively pulsed sputtering. The electrode employs an array of microtips that penetrate the outer skin layer (i.e. *stratum corneum*) that is 10 µm thick. The microtips (100-200 µm deep) were micromachined through a bulk-micromachining process based on a KOH solution.**

***Keywords: dry electrodes,* IrO_x electrode.**

I - Introduction

The electrodes are key elements for acquiring EEG signals. The high demand on non-invasive EEG electrodes for monitoring, diagnostics and treatment of patients with neural diseases, such as epilepsy, is driving the research of electrodes fabricated in different materials and with very low impedance.

The Ag/AgCl standard electrodes present a low impedance in the interface skin-electrode and good stability through its life span. However, these electrodes require a previous preparation in the outer skin (i.e. *stratum comeum*) and a gel to provide a good contact between electrode and skin to minimize the insulating effect of the *stratum comeum* layer. The standard Ag/AgCl gel electrodes have limited use because they suffer from dehydration, which leads to a modified electrode impedance and consequently, generates noise and other artifacts in the measured signals. Furthermore, the gel can cause skin irritation and support bacterial growth [1]. A dry Ag/AgCl electrode was proposed for acquiring biopotentials with promising results [2]. Nevertheless, despite the good electrochemical characteristics, the AgCl is toxic and presents an infection risk because it dissolves in contact with the skin [3].

This paper presents a non-invasive dry electrode for EEG. The brain electrical activity occurs between neurons as well as in muscles. The neuroscience field has been demanding invasive electrodes that are implanted in single and multiple recording sites [4]. Electrodes with microtips are presented in Figure 1(b). The microtips length is about 100-200 µm for providing the penetration of the outer skin layer (i.e. *stratum corneum*) that is 10 µm thick.

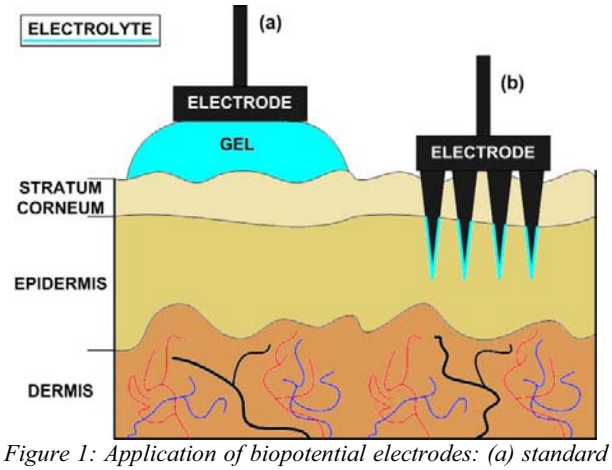

Figure 1: Application of biopotential electrodes: (a) standard EEG electrode; (b) EEG dry electrode with microtips.

II – Design

The design of the dry electrode consists in a pyramidal structure. The penetration of the microtips in the skin requires a specific pressure [5]. The pressure in the microtip, when an axial load is applied, is given by:

$$P = \frac{F}{A} \tag{1}$$

where P is the pressure resulted in the solid structure (i.e. microtip), F, the perpendicular force applied, and A, the section where the force is applied. The force necessary to insert and remove the electrode is about 10 N [5]. The Figure 2 shows the pairs of action-reaction forces, established in the electrode when inserted in skin (the distribution of the force is uniform on the electrode through the 4x4 microtips array - 0.625 N per microtip). The base of the microtip structure is subjected to a pressure of 15.6 MPa. Therefore, every microtip achieves a maximum pressure endured by silicon at 165 µm from the base (red section in Figure 2). The average height of the pyramidal structures is about 200 µm.

III – Fabrication

A. Etching

Each microtip in the dry electrode has a three dimensional structure, which is fabricated by a wet-etching process in silicon through a liquid solution of potassium hydroxide (KOH). The microtips desired shape is obtained by the undercut effect in the etching, where the planes of fast etching are revealed. It was used a [100]-type silicon wafer with a thickness of 500 µm. Also, two layers of silicon nitride (SiN) on the top and on bottom were used as masks for the etching. The Figure 3 shows the microtips fabrication steps.

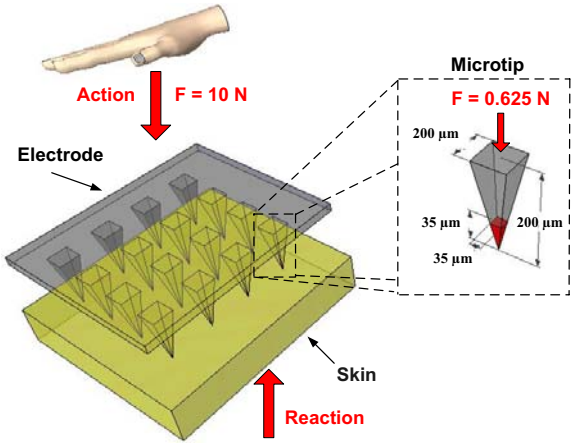

Figure 2: Pairs of action-reaction forces on a electrode with an array of 4x4 microtips.

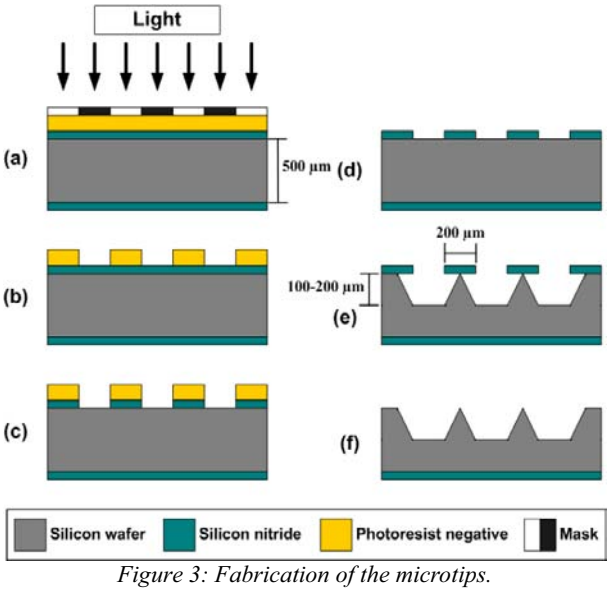

Figure 3: Fabrication of the microtips.

In the Figure 3(a), a mask, with 200 µm square openings, was used to define the microtips by lithography process. The photoresist was removed in the second step (b) from the uncovered areas. Then, the opened window in the SiN layer allowed the exposition to its elimination in the third step (c) whereas the photoresist is removed afterwards (d). The Si wafer is etched during the step (e). The remaining areas with SiN worked out as a protection layer for the etching process of the Si wafer. The etching solution of KOH was by 30% at a temperature of 87 ºC, ensuring an etching rate of 1.6 µm/min. Finally, the remaining layer of SiN was removed (f).

B. IrO_x Sputtering

The iridium oxide (IrO_x) electrodes were deposited by means of pulsed magnetron sputter using Ar/O_2 plasma prior to which, a Ti adhesion layer (with a thickness of 50 nm) was deposited on the substrate [6]. The IrO_x resistance in a 270 nm thick film was 349×10^{-6} Ωcm. The film thicknesses were determined via liftoff process with a *Tencor Pa-10* profilometer. The thin film resistance was measured in a classic four-point probe system.

IV – Experimental Results

A. Electrode Microtips Fabrication

The Figure 4 shows the emerged microtips by optical microscopy every 30 minutes through the undercut effect on the etch process.

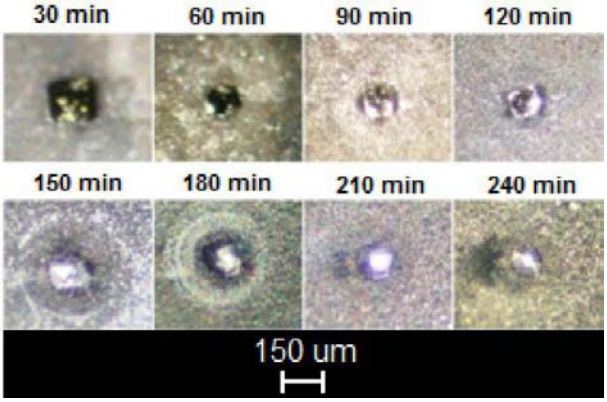

Figure 4: Top view of etching progression stages with 30 minutes intervals.

The etching process employed is anisotropic, with an angle of 54.7º between the [111] and the [100] planes. The microtip pyramidal structure due to the anisotropic process is presented in the Figure 5. One can observe the etching of square corners to an hexagonal shape as its final structure. The final microtip was 150-200 µm wider with a height around 100-200 µm.

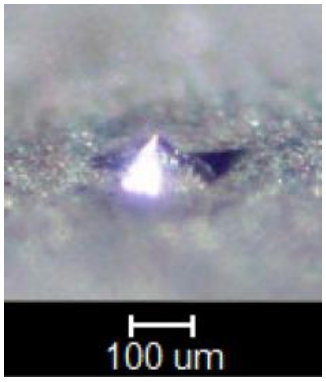

Figure 5: Microtip structure with a pyramidal shape.

B. Electrode Characterization

The deposition sessions were done in a *Nordiko NS 2550* sputtering system and pulse generator *ENI RPG-100* at 180 W. The plasma uses argon (Ar) at 100 sccm of flow with a pressure of 10^{-4} Pa. The target of pure iridium (Ir) has a resistivity of 5.3×10^{-8} Ωm.

The Table 1 lists the characteristics of the thin-films made of IrO_x. The resistivity of the thin-films is one of the main characteristic for determining the quality of the electrode, and it was measured via the *van der Pauw* method [7].

Table 1: *The session parameters in the sputtering depositions at frequency of 50 kHz.*

O_2 flow (sccm)	2	3.5	6.5	10
Deposition rate (nm/min)	13.5	14	33	28
Thickness (nm)	265	349	526	199
Resistivity ($\Omega m \times 10^{-7}$)	1.926	1.664	2.487	4.914

It would be expected that the increase of O_2 would result in an increase of the films resistivity. Such result would be expected as the increase of O_2 decreases the film purity. However, around 3.5 sccm of O_2, a lower film resistivity was obtained.

The SEMs in the Figure 6 may induce a justification for the lower resistivity at 3.5 sccm of O_2 flow.

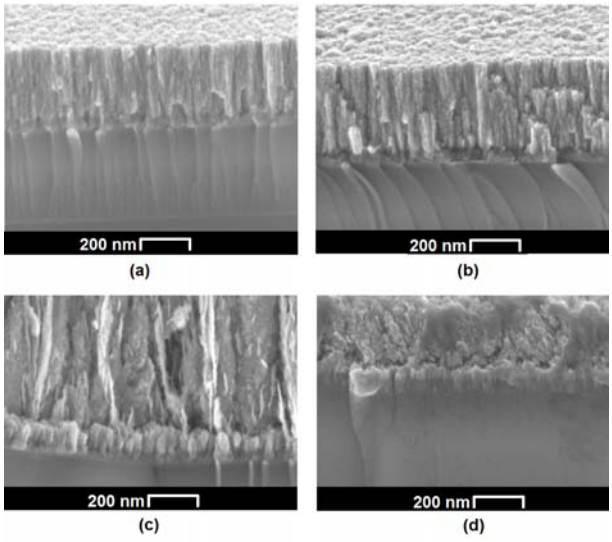

Figure 6: SEM images in cut-view of IrO_x thin-film deposited at different O_2 flows: (a) 2 sccm; (b) 3.5 sccm; (c) 6.5 sccm; (d) 10 sccm.

Apparently, the transition point between stable and unstable thin-film structures happens with an O_2 flow around 3.5 sccm. It appears that in the region of this O_2 flow, the film permittivity increases ensuring lower resistivity than the other samples. Under this flow, the structure is very consolidated which leads to an increased resistivity. Above this flow, the irregular surface induces the highest resistivity obtained. Consequently, 3.5 sccm was the selected flow for coating the electrodes under evaluation.

The O_2 in IrO_x allows the utilization of these electrodes for other application besides recording. As IrO_x has four states of oxidation in reversible chemical reactions, it enables functional stimulation [8].

The Figure 7 shows the variation of current density versus the applied voltage in the IrO_x thin-films when submerged in a NaCl solution with 0.9 % concentration.

These results allow the evaluation of the electrical activity for stimulation of the IrO_x dry electrodes. The results showed good electrochemical properties for 2 and 3.5 sccm O_2 flows.

The charge capacity versus the O_2 flow was plotted in Figure 8. The maximum charge capacity occurs for 3-4 sccm of O_2 flow, for a sputtering frequency of 50 kHz.

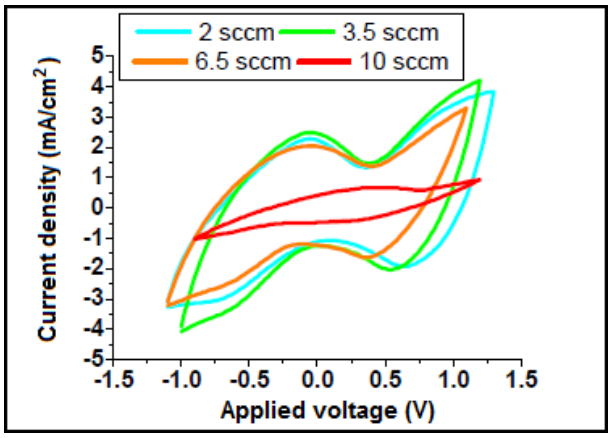

Figure 7: Current density vs. applied voltage for four different O_2 flows at 50 kHz sputtering frequency.

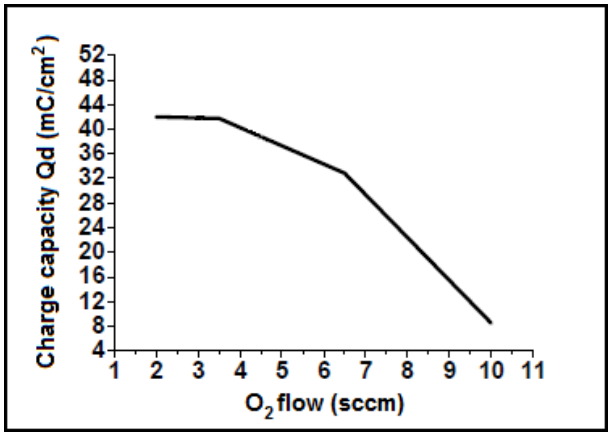

Figure 8: Comparison between charge capacity vs. O_2 flow at 50 kHz.

V – Conclusions

This paper proposes a non-invasive IrO_x dry electrode for EEG acquisition fabricated in bulk-micromachining technology. This electrode can avoid the skin preparation with gel due to its microtips structure, which penetrates through the *stratum corneum* layer.

After the fabrication and the characterization of the electrodes, the optimum deposition conditions were obtained for O_2 flows between 2-3.5 sccm and at 50 kHz sputtering frequency. Also, the developed microtips showed a good mechanical behaviour and strength to penetrate the skin.

The iridium oxide had an excellent overall performance not only for biopotential recordings but also functional stimulation application due to charge delivery capacity, low-constant transition impedance and low-resistivity. Thin-films made of IrO_x demonstrated long-term mechanical stability and good corrosion resistance.

Acknowledgments

The authors would like to thanks the Portuguese Foundation for Science and Technology for sponsoring the project FCOMP-01-0124-FEDER-010909 (refª. FCT/PTDC/SAU-BEB/100392/2008) and the company IVV AUTOMACAO LDA.

References

[1] A. Searle and J. Kirkup, “A direct comparison of wet, dry and insulating biolelectric recording electrodes”, Physiological Measurement, Vol. 21, pp. 271 – 283, 2000.

[2] P. Griss, H.K. Tolvanen-Laakso, P. Meriläinen, and G. Stemme, "Characterization of micromachined spiked biopotential electrodes", IEEE Transactions on Biomedical Engineering, Vol. 49, pp. 597-604, 2002.

[3] T.C. Ferree, P. Luu, G.S. Russell, and D.M. Tucker, "Scalp electrode impedance, infection risk, and EEG data quality", Clinical Neurophysiology, Vol. 112, pp. 536-544, 2001.

[4] A. Lebedev and M.A.L. Nicolelis, "Brain–machine interfaces: past, present and future", TRENDS in Neurosciences, Vol. 29, No. 9, pp. 536-546, July 2006.

[5] S. Henry, D.V. Mcallister, M.G. Allen, and M.R. Prausnitz, "Microfabricated Microneedles: A Novel Approach to Transdermal Drug Delivery", Journal of Pharmaceutical Sciences, Vol. 87, No. 8, pp. 922-925, August 1998.

[6] B. Wessling, W. Mokwa, and U. Schnakenberg, “RF-sputtering of iridium oxide to be used as stimulation material in functional medical implants”, Journal of Micromechanics and Microengineering, Vol. 16, pp. 142–148, 2007.

[7] L.J. van der Pauw, "A method of measuring the resistivity and Hall coefficient on lamellae of arbitrary shape", Philips Research Reports, Vol. 20, pp. 220-224, 1958.

[8] E. Slavcheva, R. Vitushinsky, W. Mokwa, and U. Schnakenberg, "Sputtered iridium oxide films as charge injection material for functional electrostimulation", Journal of the Electrochemical Society, Vol. 151, No. 7, pp. 226-237, May 2004.